Hyperspectral Remote Sensing in China

TONG Qingxi* ZHENG Lanfen
The Institute of Remote Sensing Applications, Chinese Academy of Sciences. P.O. Box 9718, Beijing 100101, China
XUE Yongqi
The Shanghai Institute of Technical Physics, Chinese Academy of Sciences. 500 Yu Tian Road, Shanghai 200083, China
ZHANG Bing, ZHAO Yongchao, LIU Liangyun
The Institute of Remote Sensing Applications, Chinese Academy of Sciences. P.O. Box 9718, Beijing 100101, China

ABSTRACT

In recent years, hyperspectral remote sensing has stepped into a new stage in China. There are some advanced hyperspectral imagers and CCD cameras developed by Chinese institutes and companies. Pushbroom Hyperspectral Imager (PHI) and Operative Modular Imaging Spectrometer (OMIS) have presented the level of airborne hyperspectral imagers in China, Which have been developed by the Chinese Academy of Sciences. A narrow band hyperspectral digital camera system (HDCS) was developed and tested in 2000, the center of wavelength of which can be changed to fit different applications. There is also a kind of Fourier Imaging Spectrometer developed in China. Accordingly, Chinese scholars have created a number of models to meet different application problems. Some new models for hyperspectral remote sensing are provided. They are Hyperspectral Data Classification Model, POS Data Geometric Correction Model, Derivative Spectral Model (DSM), Multi-temporal Index Image Cube Model (MIIC), Hybrid Decision Tree Model (HDT) and Correlation Simulating Analysis Model (CSAM). Some successful applications are provided and evaluated.

Keywords: Hyperspectral imager, Remote sensing, Model, Development

1. INTRODUCTION

For rapid progress in hardware facture, hyperspectral sensors have made great strides in the late few years in China. In airborne hyperspectral sensors, based on IR/UV, VIS/MIR/IR, FIMS, ATIMS, MAIS, China has developed Push-broom Hyperspectral Imager (PHI) and Operative Modular Imaging Spectrometer (OMIS), which have won well appraisements. In airborne CCD cameras, IRSA,CAS has designed a narrow band hyperspectral digital camera system (HDCS) designed and implemented for real-time environmental and agricultural monitoring. Also, a large aperture static interference imaging spectrometer (LASIS) was developed by Xi'an institute of optics and precision mechanics, CAS, in 1999. Furthemore, a new static interfering Fourier transform imaging spectrometer (SIFTIS) will also be developed in 2001, which is designed for aerial application.

With the development and perfection of the hyperspectral remote sensing technologies, hyperspectral remote sensing has been the major technique applied in many studies. For hyperspectral sensors have become available to provide both high spatial and high spectral resolution with high signal/noise ratio. Due to the sufficient spectral features such as spectral reflectance with wavelength it provides, hyperspectral data plays an important role in the different fields. So it is a rush now to develop some special algorithms and models for hyperspectral data processing, information extraction, classification and identification.

In the field of vegetation study especially for precise agriculture, some successful progresses are already achieved. They are the works of Tanvir[1], Chadbum[2], et al.[3, 4, 5, 6] by using derivative spectral analysis model for background noise elimination, "red edge" determination or biochemical parameter detection. Another attempt is to search all kinds of

* Tqx@hrs.irsa.ac.cn ; phone 86 10 64870569; fax 86 10 64889210; http://page.irsa.ac.cn; Institute of Remote Sensing Applications Chinese Academy of Sciences.

Multispectral and Hyperspectral Image Acquisition and Processing, Qingxi Tong, Yaoting Zhu, Zhenfu Zhu, Editors, Proceedings of SPIE Vol. 4548 (2001) © 2001 SPIE · 0277-786X/01/$15.00

spectral parameters or parameter combinations to build reliable relationship with biochemical parameters such as LAI[7, 8]. Furthermore, special angle mapper (SAM) model is also proved to be effective[9, 10]. However, there still are many difficulties due to the unique spectral features of vegetation as: **1**). The spectral shapes of all vegetation are somewhat similar while the spectra of a same species vary remarkably and therefore it is very difficult to classify using the usual method for multi-band image; **2**). Vegetation is active with a high dynamic and therefor it has a strong spatial and temporal variation; **3**). Usually it is a mixed spectrum and is strongly effected by many kinds of background even the weather; **4**). The influencing factors and their effects are very complicated; **5**). The effect of pixel size is somewhat conspicuous. Therefore, new model to consider the complex, mixed, dynamic and temporal properties of vegetation spectrum must be studied and developed to promote the better application of hyperspectral remote sensing in vegetation detection.

The purpose of this paper is to provide some new models for hyperspectral remote sensing in China. They are Hyperspectral Remote Sensing Data Classification Model, POS Data Geometric Correction Model, Derivative Spectral Model (DSM), Multi-temporal Index Image Cube Model (MIIC), Hybrid Decision Tree Model (HDT) and Correlation Simulating Analysis Model (CSAM).

2. TECHNICAL DEVELOPMENT

2.1 Airborne Hyperspectral Imager

Following the world foreland of remote sensing, two kinds of applied and commercial hyperspectral imagers were built in China in 1990s.One imager is Operative Modular Imaging Spectrometer (OMIS). In contrary to the previous imaging system OMIS has the ability acquire the images of earth's surface in three continuous reflectance spectral regions and two emission spectral regions. The linear array detectors with the optic-mechanical scanning system is adopted for OMIS. This imager is made up of five parts, which are optic-mechanical system, Real-time calibration system, electronics system, Real-time data recording and monitor system, gyro stable flat system and GPS orientation system. It can focus on the same pixel well in different band from the visible region to thermal infrared region. The other imager based on the area array CCD and pushbroom technology is Pushbroom Hyperspectral Imager (PHI). A solid state area array silicon CCD device of 780×244 elements is used as the detector of PHI. PHI has three parts: optic-mechanical system, signal process box and industrial control computer. This imager can acquire high spatial resolution because of its long focus time. High spectral resolution, light weight and relatively high spatial resolution, and low cost enabled these two great imagers to use widely in various fields and to fly at low altitude with light aircraft.

The two tables above present the parameters of PHI and OMIS respectively.

Total bands: 128	FOV: > 70°
64,32,16 optional bands in 0.4~1.1 µm	Scan rate: 5 line/s,10 line/s,15 line/s,20 line/s
16,8,1 optional bands in 1.1~2.0 µm	Pixel /line: 512,1024
32,1 optional bands in 3.0~5.0 µm	Data code: 12bit
8,1 optional bands in 8.0~12.5 µm	Data rate: 81.92 Mbps
Spectral resolution: 10nm in 0.4~1.1 µm	linear array Detector: Silicon in 0.4~1.1 µm
30nm in 1.1~2.0 µm	Indium, gallium, arsenic in 1.1~2.0 µm
15nm in 2.0~2.5 µm	Stibium, indium in 2.0~2.5 µm
250nm in 3.0~5.0 µm	Stibium, Indium in 3.0~5.0 µm
500nm in 8.0~12.5 µm	Te, cadmium, Hg in 8.0~12.5 µm
IFOV: 3 mrad,1.5 mrad	Gyro stable flat angle precision: 5'

Table 1: OMIS parameters table

CCD 244 bands	Data rate: 14 MB/Sec
FOV: 0.36rad(21°)	Weight(head): 9 kg
IFOV: 1.5mrad	Frame rate: 60 Fr/Sec (Maximum)
S/N: 300	PC plus port: ISA
Spectral region: 400nm-850nm	RAM address: (Hex)D000:0-D000:ffff
spectral resolution: <5nm	Port:(Hex)300
Spatial sampling: 376pixel/line	IRQ: 5

Table 2: PHI parameters table

2.2 Narrow Band Hyperspectral Camera

For rapid and steady collection of high spectral resolution airborne data, a narrow band hyperspectral digital camera system (HDCS) was developed and tested in 2000 by Institute of Remote Sensing Applications Chinese Academy of Sciences. The HDCS was built based on three 1024x1024 pixels, 12bits digitalized area CCD cameras, FOV and IFOV of which are about 20 degree and 0.34 mrad respectively. Precise exposure control and synchronic trigger control are provided in this system, and the problem of collection and recording of large digital image data has been well solved.

The center wavelength and bandwidth of the bandpass optical filters in this system can be customized to fit different application. The filter bandwidth can be changed from 10 to 25nm, and the filter center wavelength can be changed from 400nm to 900nm. The 10nm bandpass filters centered at 555, 650, 725nm and 650, 725, 825nm were used for agriculture research in the test phase. High spatial-resolution hyperspectral images were acquired on December 5, 2000 with the HDCS. At an altitude of approximately 3500 meters, the spatial resolution was 1.2 meter. Image processing was made for improvement of the image quality.

The panchromatic image (Fig 2a) seems very clear. However, the narrow band image (Fig 2b) is rather smearing. Because the energy of incoming light passed through 10nm interference filter was very low, proper exposed narrow-band images were captured by means of increasing the exposure time to 90ms. And the flight speed of the jet plane was about 120 meters per second. So the motion-blur problem rose. And the motion-blur extent is about 9 pixels. Figure 2d demonstrates the deblurred images using Wiener filter method with window techniques [11]. Figure 2d is a motion deblured image of figure 2b. It is much clear than figure 2b. Figure 2c is a three-band false-color image registered from three motion-deblured images (R725nm, G650nm, and B555nm). From figure2d, we can see the effect of restoration is overall very good except a little enlargement of noise.

The most useful feature of this system is its low overall cost and its flexibility to meet user needs. Because it is mounted in a small airplane, the HDCS can be flown over specific regions at varying altitudes to produce whatever spatial and temporal resolution. Researchers can now obtain hyperspectral data when and where they want it instead of being limited by relatively rigid imaging schedule of satellite. Users can do their hyperspectral band selection according to their application. And then, the only modification of the HDCS is to change the filters to fit the customized bandwidth and center wavelength.

2.3 Fourier Imaging Spectrometers

There are also other kinds of imaging spectrometer made in China. A large aperture static interference imaging spectrometer (LASIS) was developed by Xi'an institute of optics and precision mechanics, CAS, in 1999. The Fourier transform imaging spectrometer collects interferogram of the hyperspectral image cube. If the interferogram is Fourier transformed, we can acquire the spectral. The LASIS's most attractive advantages is high-throughput and high-stability. A COHU 4912 array CCD is employed, the imaging spectrometer's focus length is 80mm. The FOV and IFOV are 3.16° and 0.1mrad respectively. The SIFTIS spectral range is from 0.486 to 0.75μm, and its spectral resolution is $150cm^{-1}$.

Furthermore, a new static interfering Fourier transform imaging spectrometer (SIFTIS) will also be developed in 2001, which is designed for aerial application. The SIFTIS's FOV and IFOV are 11.5° and 0.2mrad, and the spectral range is from 0.45 to 0.9 with 256 spectral channel.

3. HYPERSPECTRAL MODEL DEVELOPMENT AND APPLICATIONS

3.1 Hyperspectral Remote Sensing Data Classification Model

Many materials can be identified by unique absorption feature in their reflectance spectra. Consequently, hyperspectral image have been so widely used in the mineral mapping, vegetation classification and environment analysis, etc. Due to the complicated urban scene and relative disorder earth object in city, it is not easy to get a satisfactory classification result only depending on pixel-to-pixel spectral analysis, especially when the materials lacked strong absorption features and the remote sensing data have a low signal-to-noise ratio [12]. However, there are always very large requirement for urban mapping, particularly in China, whose city scene have been changing with almost each passing day. The airborne hyperspectral remote sensing technology can pay an important role in the urban landcover survey, particularly for the classification based on material composition difference.

This new method for classifying hyperspectral remote sensing data in urban area is described in this section, that combines the edge detection and spectral analysis together. Due to the varied surface scene in city and limitation of imaging spectrometer's signal-to-noise ratio, normal classification based on pixels were not satisfied for thematic classification and mapping in urban area. Comparing with the classification on individual and isolated pixels, this classification on spectral polygons provides a great improvement of landcover mapping results in Beihai city. Because the appearance of the objects has been extracted from digital photographic data, the continuous spectral classification will not decompose the integration of object-classes. This is very important for the hyperspectral data usually with low signal-to-noise ratio and low spatial resolution. In addition, the spectral mean square deviation between different polygon-classes is larger than the deviation between different pixel-classes. Apparently, this approach has the advantage of increasing the diversity of different classes of spectra, which improve the accuracy of spectral classification. This technology could meet with the need of urban mapping in large scale.

3.2 POS Based Correction Model

Technology of airborne remote sensing is widely used in agriculture, geology, urban management and many other spheres. However, the problems of images' quality stunt its development all along. Because the latitude of flying plane is low enough to be affected by air currencies, it is a challenge to keep flight flying stably, even if stable platform is put into use. As a result, airborne remote sensing images have more distortions and worse quality than images of satellite images. We have no high precise parameters and coefficients in airborne remote sensing system till now [13]. Usually, airborne images' correction is done by registration of ground control points. This method needs too much ground work and cost a lot. It is not feasible well. Position and Orientation System / Direct Georeferencing (POS/DG) data is important to hyperspectral images, for it has much information of flight attitude, such as absolute position (x,y,z) and platform attitude parameters, which make it possible for geometric correction of airborne images with receiving POS/DG data. It can save much work and the cost of stable platform. It is an attempt in China that remote sensing images are corrected with airborne POS/DG data. Attached drawing figure 1 image a is a PHI raw image, image b is the one after geometric correction and resampling, and image c is the course drawn by POS/DG data. Comparing the image a、b、c, we can see that the problems of wandering, pitching and rolling are solved by POS/DG data. Corrected image moves along with the course completely; stretch and distortion are well resiled. Both distorted roads and ridges of field come back to be beelines.

3.3 Derivative Spectral Model (DSM)

The use of derivative spectra is an established technique in analytical chemistry for eliminating background signals and for resolving overlapping spectral features. In remote sensing, the detection and estimation of ground features by reflectance spectroscopy of the earth suffers from analogous interference by background signals and contributions from other targets in the view of the remote sensor. For example, varieties of soil background reflectance interfere to the estimation of crop growth condition or yield. Attenuation within the atmosphere is also a major concern. With the development of hyperspectral imaging spectroscopy, the technique of spectral derivative is widely used in high-resolution spectral research of remote sensing[14]. Due to the spectral sampling of remote sensor being discrete, differentiation is usually used to approximate the derivative spectra. That is, divide the difference between successive spectral values by the wavelength interval separating them. The equation is

$$R'(\lambda_i) = \frac{R(\lambda_{i+1}) - R(\lambda_{i-1})}{\lambda_{i+1} - \lambda_{i-1}}, \qquad (1)$$

where R' is the first order derivative of reflectance, R is reflectance, λ is wavelength, i is the channel number.

In a composite soil-vegetation spectrum, soil spectrum tends to appear low frequency noise with roughly a linear expression, while vegetation spectrum appears high frequency with roughly a polynomial expression. Thus with derivative order increasing, the soil contribution could be eliminated gradually from the composite spectrum and vegetation information of interest preserved.

Derivative treatment can also be used to locate the "red edge" of vegetation[15], so that many researchers could study the "red edge" in relation to biophysical or biochemical content or its change[16, 17]. Another important use is its effect in the resolution of overlapping spectra[18], which is quite useful for classification. Jinnian Wang[10] used derivative spectral matching algorithm for vegetation classification for Poyang Lake wetland, China, and got quite satisfactory result.

3.4. Hybrid Decision Tree Model (HDT) for classification

According to the rice spectral features of hyperspectral image data acquired during the rice is growing, a hybrid decision tree classification algorithm dealing with the variety of rice is developed. The decision tree is defined as a classification procedure that recursively partitions a data set into smaller subdivisions according to a set of tests defined at each branch node in the tree. The tree is composed of many nodes, a set of inter-nodes (splits), and a set of terminal nodes (leaves). Each node in a decision tree has only one parent node and two or more descendant nodes[19]. A data set is classified according to the decision framework defined by the tree; a new class label is assigned to each object according to the leaf node into which the object falls. There are three sorts of decision tree. That is, univariate decision tree, multivariate decision tree and hybrid decision tree. Among them, hybrid decision tree is the most complex and flexible, where different classification algorithms can be used in different subtrees of a larger tree. So in principle, the hybrid decision tree should be more precise and more effective than the other two[20], which was verified in the study. The feature bands are selected according to the separability among bands, but the classification algorithm is selected according to its classification result. The separability among bands is calculated by the normalized mean value of each band. In the end, a classification experiment is done. In the experiment the hyperspectral image data acquired in Jintan rice breeding farm is used. A good classification result is achieved. The classification accuracy of test samples is reached 94.9 percent. Another classification test is based on OMIS data (128 spectral bands, acquired in Yayunchun, Beijing) under this model. Several spectral bands which are more sensitive to the building materials (metal, plastic, sand, cement etc.) were extracted for such objects identification.

3.5. Vegetation pigments extraction and dynamic analysis

Since new hyperspectral sensors now have become available to provide both high spatial resolution and high spectral resolution data. These characteristics combined with high signal to noise ratio allow that more possible to differentiate vegetation types and extract biophysical or biochemical information which are of great importance for precision crop management.

For the detection of vegetation pigment content per unit area, two main approaches are widely used, one focus on the narrow bands ratios, including ratios within visible and near-infrared region[21], ratios only in the visible region and ratios in the red edge region [22,23,24]. The other approach utilizes the characteristics of the first and second derivatives of reflectance spectra. The majority of researchers use the wavelength position of the red edge as the best predictor of chlorophyll [25,26], while others prefer to the amplitude of the first and second derivatives of reflectance at particular wavelengths[27.28]. Some studies identify, when predicting chlorophyll content, first derivative spectra value can get same results with ratio vegetation index (RVI). Apart from pigment, LAI and percent cover were related to ratios of reflectance in narrow bands on the near-infrared plateau and red edge features of canopy reflectance spectra, as well as with the amplitude of the first derivative in the red edge and visible regions respectively[27.29]. Some water absorption peaks (e.g. 970nm) were found useful to estimate the leaf water content[30]. Fouche[31], found that the single narrow band wavelengths 707nm and 589nm provide the better nitrogen (N) applications detection at different N-levels, based on the balloon hyperspectral image data with 8 filters digital camera. Chlorophyll contents map and leaf senescence are separately shown in figure3, figure4. The airborne hyperspectral data was acquired in Changzhou by Pushbroom Area-array Hyperspectral Imager in high spectral resolution (less then 5nm). Especially, all the maps were achieved only by several channels. By this token, hyperspectral CCD camera with limited channels can play an important and independent role in the crop growth investigations.

In August, 2000, a set of reflectance spectra were gathered for two kinds of vegetables, eight distinctive growth stages for lettuce and seven for Japanese cabbage in Minamimaki area, Japan. The spectra were measured by an ASD FieldSpec FR spectroradiometer, which records a continuous spectrum between 350nm and 2500nm with a nominal sampling interval of 3nm (350-1000nm) and 10nm (1000-2500nm). Fig. 5 shows the dynamic curve of each physiological index. In order to display the dynamic trend of all the indices in the same coordination, all the indices are normalized by the average of the corresponding eight or seven stages. These temporal index curves diagnostically embody pigment and biophysical parameters in crop periods of duration.

3.6. Correlation Simulating Analysis Model (CSAM)

The study shows that the Correlation Simulating Analysis Model (CSAM) is effective to crop species discrimination[32, 33]. In order to show the correlative difference of shape between different spectral curves, it is not necessary to get the relation expression between reflectance and wavelength as $R=R(\lambda)$, where R is the reflectance and λ is the wavelength. They use a reflectance-reflectance plot which the x-axis is the reflectance of one sample (rice) and the point number equals to the band number applied. The curve so gotten is a Correlative Curve (CC) or correlative line as $R_i(\lambda)=f[R_0(\lambda)]$, where R_0 is the spectrum for X-axis and is named as Base Spectrum (BS) in this paper; f is the function of CC; i is the sample number. CSAM affords two possibilities for hyperspectral remote sensing to detect vegetation: It can magnify the difference between spectral curves, at the same time it can embody the common features of same species. Therefore, it is an ideal method for vegetation classification, and if the base spectrum (BS) is selected as a field-measured one or a standard one, it may be used as a tool for vegetation identification.

It is more important that the study shows that the relationship of PHI hyperspectral image spectra and the re-sampled field-measured spectra is also coincident with the features and rules obtained above. Therefore, classify or identification and extract bio-agricultural information by CSAM has not only theoretic but also practical reasons. Doctor Zhao also try other classification methods using general distance or general angle, the result of CSAM is the best. On the other hand, CSAM does offers a possible way to apply field spectrum in vegetation hyperspectral image processing and therefore it has an ability of identifying vegetation. CSAM also offer a potential to explore some agriculture parameters or abnormal areas. Zhao use CSAM again onto ΔR_r and try to classify the different rice breeds. The result is also good and we successfully extract the 9520 from all the rice lands that are extracted by the first-step CSAM used.

4. CONCLUSION

It is obviously that Hyperspectral Remote Sensing in China has made big strides with the advance of technique. The progress has also enhanced the demand of its applications in resources inventory and environmental monitoring. The more programs and projects conducted in the late years, the more models developed or improved for hyperspectral image processing to promote its applications. As a result, the model development can strengthen the potential of the hyperspectral imagers and expand the market of hyperspectral imager application. And also, the hyperspectral imagers will have been perfected in the courses of these applications. This has led to a positive circulation, which is the main reason why hyperspectral remote sensing is booming in recent years in China.

ACKNOWLEDGEMENTS

As a research program of the Laboratory of Remote Sensing Information Sciences, Chinese Academy of Sciences, this study is funded by the National Key Project of Science and Technology in 1996-2000, and supported by the joint research between IRSA, China and NTT Data, Japan. The development of the vegetation models were studied based on the results of the studies in the projects the National Natural Sciences Foundation of China.

We would like to thank Mrs. Miyasaki, Mr. Katsunori Kitada and Dr. Ren Fuhu for their support in this research work.

REFERENCE

1. H.D. Tanvir, D. S. Michael, "High resolution derivative spectra in remote sensing," *Remote Sens. Environ.*, **33**, pp.55-64, 1990.
2. B. P. Chadburn, "Derivative spectroscopy in the laboratory: advantages and trading rules," *Anal. Proc.*, **54**, pp. 42-43, 1982.
3. D. N. Horler, M. Dockray, J. Barber, "The red edge of plant leaf reflectance," *Int. J. Remote Sens.*, **4**, pp. 273-288, 1983.
4. I. Filella, J. Penuelas, "The red edge position and shape as indicators of chlorophyll content, biomass and hydric status," *Int. J. Remote Sens.*, **15**(7), pp. 1459-1470, 1994.
5. B. Zhang, X. Wang, , J. Liu, "Hyperspectral image processing and analysis system(HIPAS) and its applications," *Photogram. Eng. Remote Sens.*, **66**(5), pp. 605-609, 2000.
6. Q. Tong, L. Zheng, J. Wang, "Study on the wetland environment by airborne hyperspectral remote sensing," *Proceedings of the third international Airborne Remote Sensing Conference and Exhibition, Copenhagen*, **1**, pp. 67-74, 1997.
7. S. Michio, A. Tsuyoshi, "Seasonal visible, near-infrared and mid-infrared spectra of rice canopies in relation to LAI and above-ground dry phytomass," *Remote Sens. Environ.*, **27**, pp. 119-127, 1989.
8. S. T. Prasad, B. S. Ronald, E. D. Pauw, "Hyperspectral vegetation indices and their relationships with agricultural crop characteristics," *Remote Sens. Environ.*, **71**, pp. 158-182, 2000.
9. F. A. Kruse, K. S. Careen-Young, J. W. Boardman, "Mineral mapping at Cuprite, Nevada with a 63 channel imaging spectrometer," *Photogram. Eng. Remote Sens.*, **56**, pp. 83-92, 1990.
10. J. Wang, L. Zheng, Q. Tong, "The derivative spectral matching for wetland vegetation identification and classification by hyperspectral data," *SPIE*, **3502**, pp. 280-288, 1998.
11. K-C Tan, H. Lim, and B. T. Tan, Windowing techniques for image restoration. CVGIP, Vol.53, 1991, 491-500.
12. Kruse, F. A., Careen-Young, K. S., and Boardman, J. W., Mineral mapping at Cuprite, Nevada with a 63 channel imaging spectrometer, Photogram. Eng. Remote Sens, 56:83-92, 1990.
13. Xiong Zhen, Technology Search of Hyperspectral Image's Classification, p. 14～ 21, Hrs1 CAS, Beijing, 2000.

14. T. H. Shah, "Rapid non-destructive techniques for assessing crop growth rates and nitrogen status," Ph. D. Thesis, Department of Soil Science, University of Aberdeen, 1985.
15. M. Dockray,, "Verification of a new method for determining chlorophyll concentration in plants by remote sensing," M.. Sc. Thesis, Imperial Colledge, University of London, 1981.
16. B. N. Rock, T. Hoshizaki, J. R. Miller, "Comparison of the in sity and airborne spectral measurements of the blue shift associated with forest decline, " *Remote Sens. Environ.*, **24**, pp. 109-127, 1988.
17. C. Banninger, "The red edge shift as a measure of stress in coniferous forests," in abstracts of *Beltsville Agric. Res. Center Symp. XV on remote sensing for agriculture*, Beltsville Agric. Res. Center, USDA-ARS, Beltsville, Maryland. 16-18 May, 1990.
18. A. F. Fell, G. Smith, "Higher derivative methods in ultraviolet-visible and infrared spectrophotometry," *Anal. Pro.*, **54**, pp. 28-32, 1982.
19. A. Mark, Friedl, C. E. Brodley, "Decision tree classification of land cover from remotely sensed data", *Remote Sens. Environ.*, **61**, pp. 399-409, 1997.
20. M. Hansen, R. Dubayah, R. Defries, "Classification trees: an alternative to traditional land cover classifiers", *Int. J. Remote Sens.*, **17**(5), pp. 1075-1081, 1996.
21. Gitelson, Y. J. Kaufman, and M. N. Merzlyak, "Use of a green channel in remote sensing of vegetation from EOS-MODIS". *Remote Sens. Environ*. 58, pp.289-298, 1996a.
22. I. FILELLA, and J. PENUELAS, " The red edge position and shape as on indication of plant chlorophyll content, biomass and hydric status". *Int. J. Remote Sensing.* 15 (7), pp. 1459-1470, 1994.
23. A. A. GITELSON and M. N. MERZLYAK, "Signature analysis of leaf reflectance spectra: algorithm development for remote sensing of chlorophyll". *J. Plant Physical*. 148, pp. 494-500, 1996.
24. A. A. GITELSON and M. N. MERZLYAK, "Remote estimation of chlorophyll content in higher plant leaves", *Int. J. Remote Sensing*, 18, pp. 2691-2697, 1997.
25. A. A. GITELSON and M. N.MERZLYAK and H. K. Lichtenthaler, ,"Detection of red edge position and chlorophyll content by reflectance measurements near 700nm". *J. Plant Physiol*. 148, pp. 501-508, 1990b.
26. M. Mariotti, L. Ercoli and A. Masoni, "Spectral properties of iron-deficient corn and sunflower leaves". *Remote Sens. Environ*. 58, pp. 282-288, 1996.
27. G. A. BLACKBURN and C. M. STEELE, "Towards the Remote Sensing of matorral vegetation physiology: relationships between spectral reflectance, pigment, and biophysical characteristics of semiarid bushland canopies". *Remote Sens. Environ.* 70, pp. 278-292, 1999.
28. F. Boochs, K. Dockter, G. Kupfer and W. Kuhbauch, "Shape of the red edge as a vitality indicator for plants". *Int. J. Renote Sens.* 11, pp. 1741-1754, 1990.
29. J. M. CHEN, " Evaluation of vegetation indices and a simple ratio for boreal applications". *Can. J. Remote Sens.* 22, pp. 229-242, 1996.
30. J. Penuelas, J. A. Gamon, A. L. Fredeen et, al. 1994, "Reflectance indices associated with physiological changes in nitrogen- and water-limited sunflower leaves". *Remote Sens. Environ*. 48,pp. 135-146, 1994.
31. P. S.FOUCHE, E. J. BOTHA,and O. A.OGUNNAIKE, "Monitoring nitrogen response on wheat using airborne multi-spectral imaging". *21st Canadian symposium on remote sensing*, Ottawa, Canada, Ⅱ:312-325, 1999.
32. Y. Zhao, Q. Tong, et al, "Correlation simulating analysis model for crop identification", Manuscript to be published, 2000.
33. Y. Zhao, X. Zhang, Q. Tong, et al., "New Vegetation Models for Hyperspectral Remote Sensing". In: *Progress of Agricultural Information Technology*, International Academic Publishers, 2000: 294-300

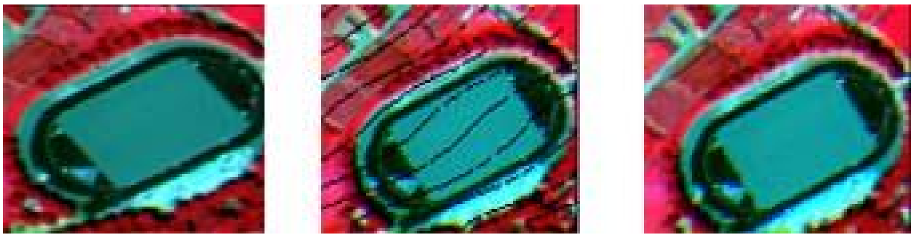

a PHI image   b Image after correction   c Image after resampling

Figure 1   part of the third course false color composite image

a

b

c

d

Figure 2. Airborne digital images captured in the test flight.
(a) Panchromatic image, exposure time 5 ms (b) 10nm wavelength bandwidth hyperspectral image, central wavelength is 650nm. Exposure time is 90ms. (c) Hyperspectral RGB false color image, R-725, G-650, B-555nm. (d) Motion-deblur image of (b).

Figure 3. Chlorophyll content distributing map

Figure 4. Leaf-senescence map

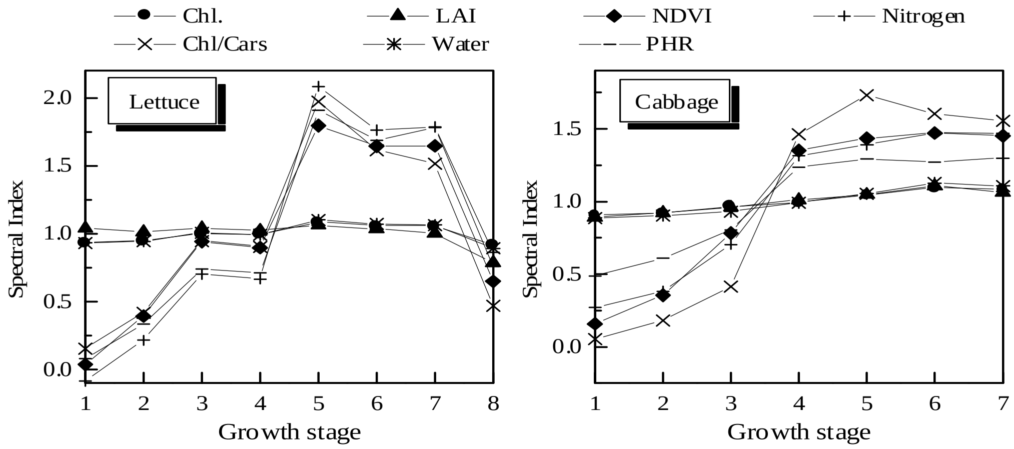

Figure5. Spectral indices change with growth stages for lettuce (left) and Japanease cabbage (right).

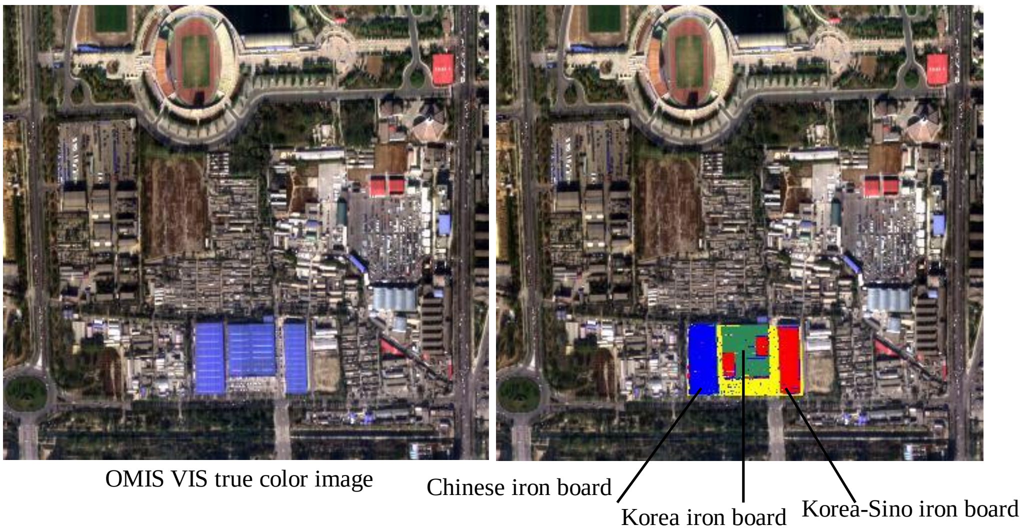

Figure 6 Iron board classification